

# Phosphate Removal by Anion Binding on Functionalized Nanoporous Sorbents

WILAIWAN CHOUYYOK, ROBERT J. WIACEK, KANDA PATTAMAKOMSAN, THANAPON SANGVANICH, RAFAL M. GRUDZIEN, AND GLEN E. FRYXELL\*

*Pacific Northwest National Laboratory, Richland, Washington 99352*

WASSANA YANTASEE\*

*Biomedical Engineering, Oregon Health & Science University (OHSU), Portland, Oregon 97239*

*Received August 14, 2009. Accepted March 11, 2010.*

Phosphate was captured from aqueous solutions by cationic metal–EDA complexes anchored inside mesoporous silica MCM-41 supports (Cu(II)–EDA–SAMMS and Fe(III)–EDA–SAMMS). Fe–EDA–SAMMS was more effective at capturing phosphate than the Cu–EDA–SAMMS and was further studied for matrix effects (e.g., pH, ionic strength, and competing anions) and sorption performance (e.g., capacity and rate). The adsorption of phosphate was highly pH dependent; it increased with increasing pH from 1.0 to 6.5, and decreased above pH 6.5. The adsorption was affected by high ionic strength (0.1 M of NaCl). In the presence of 1000-fold molar excess of chloride and nitrate anions, phosphate removal by Fe–EDA–SAMMS was not affected. Slight, moderate and large impacts were seen with bicarbonate, sulfate, and citrate anions, respectively. The phosphate adsorption data on Fe–EDA–SAMMS agreed well with the Langmuir model with the estimated maximum capacity of 43.3 mg/g. The material displayed rapid sorption rate (99% of phosphate removal within 1 min) and lowering the phosphate content to  $\sim 10$   $\mu\text{g/L}$  of phosphorus, which is lower than the EPA's established freshwater contaminant level for phosphorus (20  $\mu\text{g/L}$ ).

## Introduction

Excess phosphate in bodies of water can lead to significant eutrophication and water quality problems. Excessive phosphate results in the growth of aquatic plants, including harmful algal blooms, as well as depletion of dissolved oxygen that subsequently results in the decline of aquatic life. To control excessive growth of algae and other nuisance plants in natural water, the U.S. Environmental Protection Agency has an established a maximum contaminant level for phosphorus to be  $<20$   $\mu\text{g/L}$  in rivers and streams (1) and in lakes and reservoirs (2) during summer growing season or  $<2$  mg/L in estuarine and coastal marine waters (3). The amount of phosphate pollution has been increasing as a result of wastes generated from industrial, agricultural, and house-

hold sources. Therefore, to achieve levels below the limits set by EPA, various techniques, including chemical precipitation, biological treatment, and adsorption, have been used and studied for phosphate removal (4). While chemical precipitation is better suited at the higher phosphate concentrations encountered in some industrial waste streams, the development of adsorbents for phosphate capture has been most widely studied due to their high efficiency at low phosphate concentrations (5–7). Adsorption provides faster phosphate removal rate than does biological-based phosphate treatment. Therefore, a variety of adsorbents have been developed recently and evaluated for phosphate removal, including slag (8, 9), red mud (10), palygorskite (11), iron based components (5, 12), zirconium (13–15), coal fly ash (16, 17), crab shells (18), lithium (19), and MgMn-layered double hydroxides (20). Among these materials, lanthanum(III) plays an important role in the field of phosphate removal (6, 7, 21–23) because it is a moderately hard trivalent Lewis acid, and has a high affinity for phosphate, which is a hard base (23). The maximum adsorption capacity for those La(III) based sorbents for phosphate was reported to be about 25 mg phosphorus/g (6) but took as long as 24 h to achieve.

Self-assembled monolayers on mesoporous supports (SAMMS (a registered trademark of Steward Advanced Materials)) have been developed at PNNL over the past decade for removal of heavy metals and radionuclides from aqueous systems (24). Their extremely high surface areas and dense, ordered ligand arrays have provided high loading capacity, strong ligand binding stability, and rapid binding rate for a variety of metal chelations (25–28). It has been reported that cationic Cu(II)– and Fe(III)–EDA complexes bound to the pore walls inside mesoporous silica are capable of binding toxic anions like arsenate and chromate (26, 29–31). Additionally, Yokoi et al. (30) reported that phosphate could compete with oxyanions to bind with a Fe(III) complex, suggesting that perhaps the metal-complexes might also be effective for phosphate binding.

Therefore, we set out to study how effectively metalated EDA–SAMMS were able to capture phosphate anion from buffered aqueous media in batch contact experiments. These studies were tailored to study the effect of pH, ionic strength, and coexisting anions on phosphate capture, as well as a determination of the adsorption isotherm and phosphate sorption kinetics. This manuscript summarizes these results.

## Experimental Procedures

**Sorbent.** Two sorbent materials were used; Cu–EDA–SAMMS and Fe–EDA–SAMMS. The details of the synthesis of Cu–EDA–SAMMS were described in our previous work (26). In short, the prehydrated MCM-41 (the MCM-41 used had a specific surface area of 880  $\text{m}^2/\text{g}$ , an average pore diameter of  $\sim 30$  Å, and a pore volume of 1.29  $\text{cc/g}$ ) (32–35) was treated with ethylenediamine (EDA) terminated silane (1-(2-aminoethyl)-3-aminopropyl]trimethoxysilane) in refluxing toluene to produce EDA–SAMMS. Incorporation of the Cu(II) ions was accomplished by stirring the EDA–SAMMS in an aqueous solution of a slight excess of  $\text{CuCl}_2$  for a few hours to produce the Carolina blue Cu–EDA–SAMMS. The metalized adduct was collected by filtration, washed with water, then 2-propanol, and air-dried. Fe–EDA–SAMMS was prepared by a similar method, using a slight excess of  $\text{FeCl}_3$  in place of  $\text{CuCl}_2$ .

Elemental analysis (Galbraith Laboratories) of Cu–EDA–SAMMS revealed a mass composition of 14.41% C, 3.28% H,

\* Address correspondence to either author. Phone: (509) 375-3856 (G. E. F.); (503) 418-9306 (W. Y.). Fax: (509) 375-2186 (fax) (G. E. F.); 503-418-9311 (fax) (W. Y.). E-mail: glen.fryxell@pnl.gov (G. E. F.); yantasee@ohsu.edu (W. Y.).



**TABLE 1. Distribution Coefficients ( $K_d$ , mL/g) of Phosphate Adsorption on Fe-EDA-SAMMS and Cu-EDA-SAMMS and the Leaching of Silica and Metal Cations<sup>a</sup>**

sorbent	final pH	$K_d$ (mL/g)	silica (mg/g)	metal cation (mg/g)
Fe-EDA-SAMMS	4.6	310 000	5.18	0.06 (Fe)
Cu-EDA-SAMMS	5.8	110 000	8.96	0.92 (Cu)

<sup>a</sup> Initial phosphate concentration of ~1 ppm, liquid-to-solid ratio (L/S) of 1000 mL/g.

which presumably represents a mixture of the 1:2 and 1:3 complexes (both of which are shown in Figure 1).

Characterization of these materials by FTIR revealed the bands expected for an N-H bound to a Lewis acid metal center (broad N-H stretch from ~3700 cm<sup>-1</sup> to ~2600 cm<sup>-1</sup>, an N-H bending vibration at ~1600 cm<sup>-1</sup>, and an N-H wag at ~805 cm<sup>-1</sup>), as well as the expected C-H stretches associated with the propyl tether and EDA ligand (2970 cm<sup>-1</sup> to 2910 cm<sup>-1</sup>), and the intense broad band associated with the Si-O stretches (around 1100 cm<sup>-1</sup>) of the MCM-41 support.

The MCM-41 that we started with had a specific surface area of 880 m<sup>2</sup>/g, an average pore diameter of 30 Å, and a pore volume of 1.29 cc/g. Installation of the metalated EDA monolayers reduces all three of these values significantly, as would be expected, both from the addition of significant mass, as well as the reduction in absolute surface area due to the significant volume occupied by the metalated EDA monolayer within the pore. The Cu-EDA-SAMMS was found to have a specific surface area of 117 m<sup>2</sup>/g (as measured by BET) and a pore volume of 0.58 cc/g. Fe-EDA-SAMMS revealed a surface area of 169 m<sup>2</sup>/g and a pore volume of 0.68 cc/g. In both cases the average pore diameter was found to be less than 20 Å. These observations are all consistent with the installation of a monolayer coating throughout the nanoporous matrix, containing M(EDA)<sub>n</sub> complexes, adding mass and consuming pore volume.

The phosphate sorption performance of Cu-EDA-SAMMS and Fe-EDA-SAMMS was evaluated in term of the distribution coefficient ( $K_d$ , mL/g), which is simply a mass-weighted partition coefficient between solid phase and liquid supernatant phase as shown in eq 2:

$$K_d = \frac{(C_0 - C_f) V}{C_f M} \quad (2)$$

where  $C_0$  and  $C_f$  are the initial and final concentrations of the analyte, respectively (at equilibrium),  $V$  is the volume of solution, and  $M$  is the mass of sorbent used. These initial scoping measurements were carried out in deionized water, with an initial phosphate concentration of ~2 ppm (in the form of KH<sub>2</sub>PO<sub>4</sub>). The liquid-to-solid ratio was 1000 mL/g. These comparative results are summarized in Table 1. According to Pearson's hard soft acid base theory (37), Fe(III) ion is a "harder" Lewis acid than is Cu(II) ion. As a result, Fe(III) is able to bind phosphate (a hard base) more strongly than Cu(II) ion (similar results were obtained by Yoshitake and co-workers for arsenate anion (30)). In addition, Fe-EDA-SAMMS leached less metal ligand and silica than did Cu-EDA-SAMMS. Therefore, Fe-EDA-SAMMS was chosen for further evaluations for the matrix effects (pH, ionic strength, and other anions) as well as the phosphate sorption capacity and rate.

**Adsorption Isotherm.** In order to determine the maximum adsorption capacity of Fe-EDA-SAMMS for phosphate, the adsorption isotherms were measured in DI water containing different concentrations of phosphate (pH ~ 5)

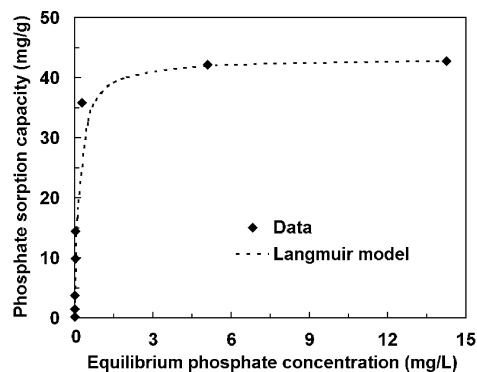


**FIGURE 2. Adsorption isotherm of phosphate on Fe-EDA-SAMMS in DI water (pH 5.0), L/S of 10 000 mL/g, symbols represent data, and dash-line represents Langmuir isotherm fitting.**

and at liquid-to-solid ratio of 10 000 mL/g. The adsorption isotherm data fit the Langmuir adsorption model well, as shown in Figure 2 ( $R^2 > 0.99$ ), indicating the adsorption of phosphate anions is taking place in a monolayer fashion. The adsorption capacity of phosphate increased with increasing equilibrium phosphate concentration and reached a maximum once the equilibrium phosphate concentration approaching 5 ppm, indicating the adsorption sites were saturated. The maximum adsorption capacity of phosphate was 43.3 mg (0.46 mmol) per g of Fe-EDA-SAMMS. At a functional loading of 0.83 mmol Fe(III) per gram of sorbent, it appears that a little over half of the Fe(III) binding sites have been used to bind the phosphate anion (the fact that in this pH range we are dealing with the phosphate monoanion argues against the possibility of a phosphate dianion bridging between two Fe centers). This maximum phosphate capacity is significantly higher than those reported for sorbents like La doped vesuvianite (4.0 mg/g) (21), Fe oxide tailing (21.5 mg/g) (39), Fe(III)/Cr(III) hydroxide (6.5 mg/g) (12), and MgMn-layered double hydroxides (22.3 mg/g) (20), and comparable to sorbents like La/Al pillared montmorillonite (40.0 mg/g) (22), Fe-Mn binary oxide adsorbent (36.0 mg/g) (5), and commercial zirconium ferrite (39.8 mg/g) (14). For La(III) mesoporous silica, LaPO<sub>4</sub> formed during the adsorption was suspected of blocking the pores of La-based mesoporous silica (7).

Successful binding of phosphate anion with these materials raises the question of the binding mechanism by which phosphate anion is being bound: is it a simple ion exchange process (i.e., no direct bond formation between the metal center and the anion), or is it a direct coordination process (where there is a bond formed between the anion and the metal center)? Detailed XAFS studies have shown that Cu-EDA-SAMMS binds oxometallate anions like chromate and arsenate by displacing an EDA ligand from the Cu-EDA complex and forming a monodentate bond between the anion and the Cu center (38). The ability of the anion to participate in this displacement reaction has been correlated to its basicity (37). Similar XAFS studies for the Fe-EDA complex (also in mesoporous silica) binding arsenate, chromate, selenate, and molybdate anions found direct evidence of the oxoanion is bound directly to the metal center (in fact, in some cases, the authors found evidence of two arsenate anions binding to a single Fe center!) (36). Based on these precedents, and the basicity of phosphate monoanion ( $pK_b$  of 11.9), we postulate that the phosphate anion is directly bound to the Fe(III) ion of the Fe(EDA)<sub>n</sub> complex in these sorbent materials, most likely in a monodentate fashion. This raises an interesting observation: the Fe/EDA ratio observed in these materials was 1:2.2, consistent with a mixture of 1:2 and 1:3 complexes (as discussed earlier, see Figure 1), with the 1:2 complex being present at slightly higher

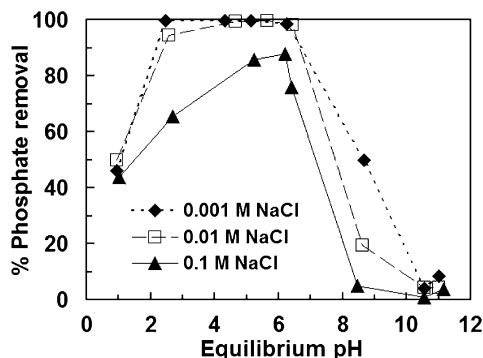


FIGURE 3. Effects of pH and ionic strength on phosphate adsorption on Fe-EDA-SAMMS in DI water, initial phosphate concentration of  $\sim 2$  ppm, L/S of 1000 mL/g.

levels. Given that only a little over half of the Fe sites are used in binding the phosphate monoanion, this suggests that only the  $\text{Fe}(\text{EDA})_2\text{X}_2$  sites enter into this binding process (see Figure 1), and that the phosphate monoanion is not sufficiently basic to displace the EDA ligand from the  $\text{Fe}(\text{EDA})_3$  complex. If phosphate binding were taking place through simple ion exchange, then either the  $\text{Fe}(\text{EDA})_2\text{X}_2$  or  $\text{Fe}(\text{EDA})_3$  complexes should be able to effectively bind the phosphate anion, but if only binding to the  $\text{Fe}(\text{EDA})_2\text{X}_2$  complex is taking place, then that is most consistent with displacement of X and formation of a direct Fe-phosphate bond.

**The Effect of pH and Ionic Strength.** The pH of solution has an impact on the speciation of the phosphate ions in solution. At pHs lower than 2.15, the predominant species is the neutral  $\text{H}_3\text{PO}_4$ . Between pHs of 2.15 and 7.20, the predominant species is  $\text{H}_2\text{PO}_4^-$ , whereas at pHs between 7.2 and 12.33 the main species is  $\text{HPO}_4^{2-}$  (40). Additionally, natural waters always contain various anions, and these coexisting ions may affect or compete with phosphate anions for the binding sites of sorbent materials. In order to assess the influence of pH and ionic strength on phosphate removal by Fe-EDA-SAMMS, the batch adsorption were investigated in solutions containing  $\sim 2$  ppm of phosphate and NaCl at varied concentrations (0.001–0.1 M) over the pH range of 1.0–11.5. The results are summarized in Figure 3. Phosphate removal increased with increasing pH from 1.0 to 6.5, and then dropped sharply as pH increased from 6.5 to 11.5. At low ionic strength (0.001–0.01 M NaCl), the maximum removal of  $>98\%$  was achieved from pH 2.5 to 6.5, while at higher ionic strength (0.1 M NaCl), the maximum phosphate removal of  $>85\%$  was achieved from pH 5.3 to 6.2. Interestingly, Fe-EDA-SAMMS was able to capture 40–50% of phosphate at pH 1, where the neutral  $\text{H}_3\text{PO}_4$  species was predominant. One possible explanation might be the protonation of the EDA ligands and anion exchange at the newly formed ammonium ion. Support for this hypothesis is found in Figure 4, where Fe is seen to leach out of the sorbent at low pH (note that no significant Si leaching was observed, indicating that the sorbent backbone or monolayer is not breaking down). It appears that this ammonium ion exchange site is not as effective as the Fe-EDA complex and the phosphate binding capacity is markedly lower at pH of 1.0 than it is at a pH of 5.0–6.0. At higher pH ( $>6.5$ ), a significant drop in phosphate removal was observed, suggesting that hydroxide anions may be competing with phosphate anions to bind with the binding sites on Fe-EDA-SAMMS (8, 14, 15). Likewise, the binding of arsenate and chromate anions at Cu-EDA-SAMMS was found to be a function of the  $\text{p}K_b$  of the anion (41). Clearly, the pH of the solution plays an important role on the adsorption of phosphate similar to a number of reports using various sorbents (that bind phosphate more effectively under acidic conditions than alkaline conditions 5–10, 12, 15, 23, 42). In contrast, there are relatively

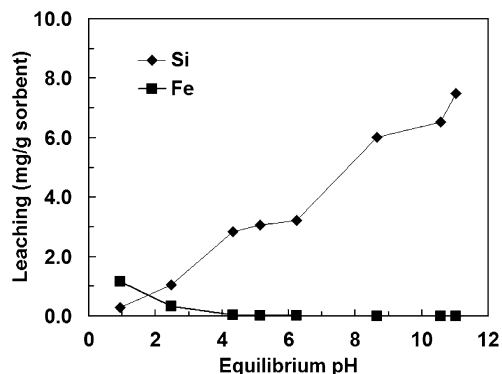


FIGURE 4. Effect of pH on Si and metal cation (Fe) leaching from Fe-EDA-SAMMS in solutions containing 0.001 M NaCl, and  $\sim 2$  ppm of phosphate, L/S of 1000 mL/g.

TABLE 2. Effect of Coexisting Anions on Phosphate Removal by Fe-EDA-SAMMS<sup>a</sup>

matrix	final pH	% phosphate removal
phosphate	4.6	99.7
phosphate +0.01 M sodium chloride	5.7	99.6
phosphate +0.01 M sodium nitrate	6.0	96.8
phosphate +0.01 M sodium bicarbonate	8.1	80.2
phosphate +0.01 M sodium sulfate	7.4	65.1
phosphate +0.01 M sodium citrate	7.2	25.9

<sup>a</sup> Initial phosphate concentration of  $\sim 1$  ppm, L/S of 1000 mL/g.

few reports (13, 14, 21) that found no significant effect on phosphate removal as pH changed from 2 to 10. Nevertheless, the results show that Fe-EDA-SAMMS would be very effective at removing phosphate in most wastes and natural waters having pH between 2.5 and 6.5 and ionic strength lower than 0.1 M.

**Effect of Coexisting Anions.** Natural waters and waste waters normally contain coexisting ions, which could potentially interfere in the binding of phosphate. Thus, the competitive sorption of the coexisting anions, including chloride, nitrate, bicarbonate, sulfate, and citrate, was studied in DI water containing  $\sim 1$  ppm of phosphate and 0.01 M of the competing anions (equivalent to 1000-fold molar excess of the phosphate). The results shown in Table 2 demonstrate that there was only small interference for the phosphate adsorption by the presence of 0.01 M chloride and nitrate anions. Phosphate adsorption by Fe-EDA SAMMS was inhibited modestly in the presence of bicarbonate and sulfate, while chelating citrate anion strongly impacted the phosphate binding. This trend agrees with the previous report that metalated-EDA-SAMMS (e.g., Cu-EDA-SAMMS) binds more basic anions more strongly than the less basic anions (41). In addition, Yoshitake found that arsenate binding by Fe-EDA was only slightly suppressed by chloride and sulfate, but Cu-EDA was substantially impacted by both chloride and sulfate, revealing an important degree of chemical selectivity of the Fe-based sorbent over the Cu-based sorbent (36). Competing anion effects on phosphate removal have also been found on other types of adsorbents (8, 14). However, for La/Al pillared montmorillonite, it was reported that phosphate removal was more strongly affected by chloride ion than by nitrate and sulfate anions (22). In light of these observations, it appears that Fe-EDA-SAMMS is well-suited for removal of phosphate in the presence of chloride and nitrate anions (which are commonly found in natural waters and a variety of common wastestreams).

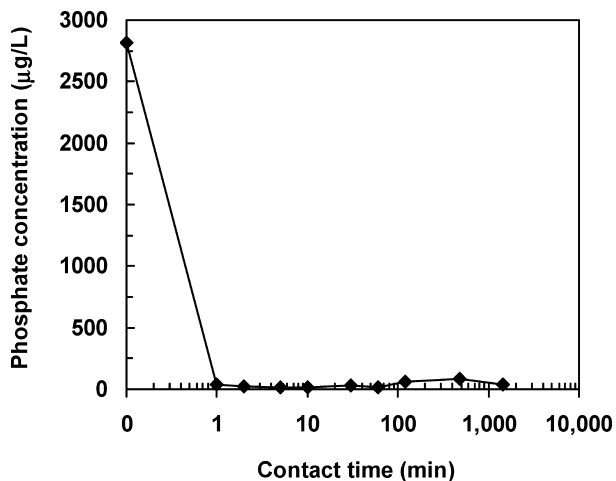


FIGURE 5. Sorption kinetics of phosphate on Fe-EDA-SAMMS in DI water (pH 5.0), L/S of 1000 mL/g.

**Adsorption Kinetics.** Adsorption kinetics plays an important role in the efficiency and field-deployment costs of a sorbent (25). Therefore, the adsorption kinetics of Fe-EDA-SAMMS for binding phosphate was studied under the same conditions as our pH studies (~2.8 ppm of phosphate and L/S of 1000 mL/g). Figure 5 shows the reduction of phosphate concentration in the solution as a function of contact time. The concentration was reduced from 2.82 ppm to 0.035 ppm (equivalent to ~99% reduction) within 1 min and remained relatively constant over the 24 h of contact time. The reaction reached equilibrium within ~1 min. Rapid phosphate sorption was facilitated by the rigid and open pore structure of the mesoporous silica, allowing easy access of phosphate anions to the binding sites. Fast sorption kinetics are highly beneficial for the rapid through-put of the phosphate-containing process stream. In comparison, the Fe-EDA-SAMMS offers much faster phosphate uptake rate than the widely studied La (6, 7, 21, 22) and Fe-based sorbents (5, 12), which normally take several hours to reach sorption equilibrium.

### Acknowledgments

This work was supported by the National Institute of Allergy and Infectious Disease (NIAID), grant no. R01 AI074064, the National Institute of Environmental Health Sciences (NIEHS), grant no. R21 ES015620, and DOE Laboratory Directed Research and Development funding. A portion of research was performed using EMSL, a national scientific user facility sponsored by the Department of Energy's Office of Biological and Environmental Research and located at Pacific Northwest National Laboratory. Pacific Northwest National Laboratory is operated for the U.S. Department of Energy by Battelle under contract DE-AC06-67RLO 1830.

### Literature Cited

- (1) *Nutrient Criteria Technical Guidance Manual: Rivers and Streams*, EPA-822B-00-002; Office of Science and Technology, U.S. EPA: Washington, DC, 2000.
- (2) *Nutrient Criteria Technical Guidance Manual: Lakes and Reservoirs*, EPA-822-B00-001; Office of Science and Technology, U.S. EPA: Washington, DC, 2000.
- (3) *Nutrient Criteria Technical Guidance Manual: Estuarine and Coastal Marine Waters*, EPA-822-B-01-003; Office of Water, U.S. EPA: Washington, DC, 2001.
- (4) Morse, G. K.; Brett, S. W.; Guy, J. A.; Lester, J. N. Review: Phosphorus removal and recovery technologies. *Sci. Total Environ.* **1998**, 212 (1), 69–81.
- (5) Zhang, G.; Liu, H.; Liu, R.; Qu, J. Removal of phosphate from water by a Fe-Mn binary oxide adsorbent. *J. Colloid Interface Sci.* **2009**, 335 (2), 168–174.

- (6) Ning, P.; Bart, H.-J.; Li, B.; Lu, X.; Zhang, Y. Phosphate removal from wastewater by model-La(III) zeolite adsorbents. *J. Environ. Sci.* **2008**, 20 (6), 670–674.
- (7) Ou, E.; Zhou, J.; Mao, S.; Wang, J.; Xia, F.; Min, L. Highly efficient removal of phosphate by lanthanum-doped mesoporous SiO<sub>2</sub>. *Colloids Surf., A* **2007**, 308 (1–3), 47–53.
- (8) Xue, Y.; Hou, H.; Zhu, S. Characteristics and mechanisms of phosphate adsorption onto basic oxygen furnace slag. *J. Hazard. Mater.* **2009**, 162 (2–3), 973–980.
- (9) Xiong, J.; He, Z.; Mahmood, Q.; Liu, D.; Yang, X.; Islam, E. Phosphate removal from solution using steel slag through magnetic separation. *J. Hazard. Mater.* **2008**, 152 (1), 211–215.
- (10) Huang, W.; Wang, S.; Zhu, Z.; Li, L.; Yao, X.; Rudolph, V.; Haghseresht, F. Phosphate removal from wastewater using red mud. *J. Hazard. Mater.* **2008**, 158 (1), 35–42.
- (11) Gan, F.; Zhou, J.; Wang, H.; Du, C.; Chen, X. Removal of phosphate from aqueous solution by thermally treated natural palygorskite. *Water Res.* **2009**, 43 (11), 2907–2915.
- (12) Namasivayam, C.; Prathap, K. Recycling Fe(III)/Cr(III) hydroxide, an industrial solid waste for the removal of phosphate from water. *J. Hazard. Mater.* **2005**, 123 (1–3), 127–134.
- (13) Yeon, K.-H.; Park, H.; Lee, S.-H.; Park, Y.-M.; Lee, S.-H.; Iwamoto, M. Zirconium mesostructures immobilized in calcium alginate for phosphate removal. *Korean J. Chem. Eng.* **2008**, 25 (5), 1040–1046.
- (14) Biswas, B. K.; Inoue, K.; Ghimire, K. N.; Harada, H.; Ohto, K.; Kawakita, H. Removal and recovery of phosphorus from water by means of adsorption onto orange waste gel loaded with zirconium. *Bioresour. Technol.* **2008**, 99 (18), 8685–8690.
- (15) Liu, H.; Sun, X.; Yin, C.; Hu, C. Removal of phosphate by mesoporous ZrO<sub>2</sub>. *J. Hazard. Mater.* **2008**, 151 (2–3), 616–622.
- (16) Guan, Q.; Hu, X.; Wu, D.; Shang, X.; Ye, C.; Kong, H. Phosphate removal in marine electrolytes by zeolite synthesized from coal fly ash. *Fuel* **2009**, 88 (9), 1643–1649.
- (17) Pengthamkeerati, P.; Satapanajaru, T.; Chularuengsookorn, P. Chemical modification of coal fly ash for the removal of phosphate from aqueous solution. *Fuel* **2008**, 87 (12), 2469–2476.
- (18) Jeon, D. J.; Yeom, S. H. Recycling wasted biomaterial, crab shells, as an adsorbent for the removal of high concentration of phosphate. *Bioresour. Technol.* **2009**, 100 (9), 2646–2649.
- (19) Wang, S.-L.; Cheng, C.-Y.; Tzou, Y.-M.; Liaw, R.-B.; Chang, T.-W.; Chen, J.-H. Phosphate removal from water using lithium intercalated gibbsite. *J. Hazard. Mater.* **2007**, 147 (1–2), 205–212.
- (20) Chitrakar, R.; Tezuka, S.; Sonoda, A.; Sakane, K.; Ooi, K.; Hirotsu, T. Adsorption of phosphate from seawater on calcined MgMn-layered double hydroxides. *J. Colloid Interface Sci.* **2005**, 290 (1), 45–51.
- (21) Li, H.; Ru, J.; Yin, W.; Liu, X.; Wang, J.; Zhang, W. Removal of phosphate from polluted water by lanthanum doped vesuvianite. *J. Hazard. Mater.* **2009**, 168 (1), 326–330.
- (22) Tian, S.; Jiang, P.; Ning, P.; Su, Y. Enhanced adsorption removal of phosphate from water by mixed lanthanum/aluminum pillared montmorillonite. *Chem. Eng. J.* **2009**, 151 (1–3), 141–148.
- (23) Wu, R. S. S.; Lam, K. H.; Lee, J. M. N.; Lau, T. C. Removal of phosphate from water by a highly selective La(III)-chelex resin. *Chemosphere* **2007**, 69 (2), 289–294.
- (24) Fryxell, G. E.; Mattigod, S. V.; Lin, Y.; Wu, H.; Fiskum, S.; Parker, K.; Zheng, F.; Yantasee, W.; Zemanian, T. S.; Addleman, R. S.; Liu, J.; Kemner, K.; Kelly, S.; Feng, X. Design and synthesis of self-assembled monolayers on mesoporous supports (SAMMS): The importance of ligand posture in functional nanomaterials. *J. Mater. Chem.* **2007**, 17 (28), 2863–2874.
- (25) Lin, Y.; Fryxell, G. E.; Wu, H.; Engelhard, M. Selective sorption of cesium using self-assembled monolayers on mesoporous supports. *Environ. Sci. Technol.* **2001**, 35 (19), 3962–3966.
- (26) Fryxell, G. E.; Liu, J.; Hauser, T. A.; Nie, Z.; Ferris, K. F.; Mattigod, S.; Gong, M.; Hallen, R. T. Design and synthesis of selective mesoporous anion traps. *Chem. Mater.* **1999**, 11 (8), 2148–2154.
- (27) Yantasee, W.; Fryxell, G. E.; Addleman, R. S.; Wiacek, R. J.; Koonsiripaiboon, V.; Pattamakomsan, K.; Sukwarotwat, V.; Xu, J.; Raymond, K. N. Selective removal of lanthanides from natural waters, acidic streams and dialysate. *J. Hazard. Mater.* **2009**, 168 (2–3), 1233–1238.
- (28) Lin, Y.; Fiskum, S. K.; Yantasee, W.; Wu, H.; Mattigod, S. V.; Vorpagel, E.; Fryxell, G. E.; Raymond, K. N.; Xu, J. Incorporation of hydroxypyridinone ligands into self-assembled monolayers on mesoporous supports for selective actinide sequestration. *Environ. Sci. Technol.* **2005**, 39 (5), 1332–1337.

- (29) Yokoi, T.; Tatsumi, T.; Yoshitake, H. Selective selenate adsorption on cationated amino-functionalized MCM-41. *Bull. Chem. Soc. Jpn.* **2003**, 76 (11), 2225–2232.
- (30) Yokoi, T.; Tatsumi, T.; Yoshitake, H. Fe<sup>3+</sup> coordinated to amino-functionalized MCM-41: an adsorbent for the toxic oxyanions with high capacity, resistibility to inhibiting anions, and reusability after a simple treatment. *J. Colloid Interface Sci.* **2004**, 274 (2), 451–457.
- (31) Yoshitake, H.; Yokoi, T.; Tatsumi, T. Adsorption behavior of arsenate at transition metal cations captured by amino-functionalized mesoporous silicas. *Chem. Mater.* **2003**, 15 (8), 1713–1721.
- (32) Beck, J. S.; Vartuli, J. C.; Roth, W. J.; Leonowicz, M. E.; Kresge, C. T.; Schmitt, K. D.; Chu, C. T. W.; Olson, D. H.; Sheppard, E. W. A new family of mesoporous molecular sieves prepared with liquid crystal templates. *J. Am. Chem. Soc.* **1992**, 114 (27), 10834–10843.
- (33) Kresge, C. T.; Leonowicz, M. E.; Roth, W. J.; Vartuli, J. C.; Beck, J. S. Ordered mesoporous molecular sieves synthesized by a liquid-crystal template mechanism. *Nature* **1992**, 359 (6397), 710–712.
- (34) Feng, X.; Fryxell, G. E.; Wang, L.-Q.; Kim, A. Y.; Liu, J.; Kemner, K. M. Functionalized monolayers on ordered mesoporous supports. *Science* **1997**, 276 (5314), 923–926.
- (35) Liu, J.; Feng, X.; Fryxell, G. E.; Wang, L. Q.; Kim, A. Y.; Gong, M. Hybrid mesoporous materials with functionalized monolayers. *Adv. Mater.* **1998**, 10, 161–165.
- (36) Yoshitake, H. Functionalization of periodic mesoporous silica and its application to the adsorption of toxic anions. In *Environmental Applications of Nanomaterials: Synthesis, Sorbents and Sensors*; Fryxell, G. E., Cao, G., Eds.; Imperial College Press: Singapore, 2007; pp 241–274.
- (37) Pearson, R. G. Hard and soft acids and bases. *J. Am. Chem. Soc.* **1963**, 85 (22), 3533–3539.
- (38) Kelly, S. D.; Kemner, K. M.; Fryxell, G. E.; Liu, J.; Mattigod, S. V.; Ferris, K. F. X-ray-absorption fine-structure spectroscopy study of the interactions between contaminant tetrahedral anions and self-assembled monolayers on mesoporous supports. *J. Phys. Chem. B* **2001**, 105 (27), 6337–6346.
- (39) Zeng, L.; Li, X.; Liu, J. Adsorptive removal of phosphate from aqueous solutions using iron oxide tailings. *Water Res.* **2004**, 38 (5), 1318–1326.
- (40) Perrin, D. D.; Dempsey, B. *Buffers for pH and Metal Ion Control*; Chapman and Hall: London, 1974.
- (41) Mattigod, S. V.; Fryxell, G. E.; Parker, K. E. Anion binding in self-assembled monolayers in mesoporous supports (SAMMS). *Inorg. Chem. Commun.* **2007**, 10 (6), 646–648.
- (42) Abou Taleb, M. F.; Mahmoud, G. A.; Elsigeny, S. M.; Hegazy, E.-S. A. Adsorption and desorption of phosphate and nitrate ions using quaternary (polypropylene-g-*N,N*-dimethylamino ethylmethacrylate) graft copolymer. *J. Hazard. Mater.* **2008**, 159 (2–3), 372–3798.

ES100787M